WELDING RESEARCH

SUPPLEMENT TO THE WELDING JOURNAL, JULY, 1982

Sponsored by the American Welding Society and the Welding Research Council

The Effects of Titanium on Submerged Arc Weld Metal

Graphs are plotted for predicting the effect of C, Mn, Si and Ti in varying amounts and combinations on weld-metal strength and toughness

BY J. P. SNYDER, II AND A. W. PENSE

ABSTRACT. The effect of titanium on the mechanical properties and microstructure of the weld metal in HSLA Si-Al-killed low-sulfur steels containing varying amounts of titanium was determined. The titanium was introduced into the weld via dilution from the base metal. The nominal C, Mn, Si and Ti ranges in the weld deposits were 0.05-0.15, 1.0-1.4, 0.35-0.60 and 0.0-0.15%, respectively. Welding was done primarily with C-Mn electrodes. The effect of flux basicity was also determined. Finally, welds were also made with C-Mn-Mo and C-Mn-Mo-Ni electrodes to determine the contribution of electrode composition to toughness.

Weld-metal yield and tensile strengths were obtained using subsize all-weld-metal tensile specimens. Toughness data were developed from standard Charpy specimens. Various microstructural features found in the weld metals were identified and quantified by means of optical and electron metallography.

The data were statistically analyzed using a two-level, three-factorial design based on C, Si and Ti and a partial factorial design based on C, Mn and Ti. Equations were developed for mechanical properties for compositions within the design limits. From these equations, a series of graphs were plotted for predicting the effect of C, Mn, Si and Ti in various amounts and combinations on weld-metal strength and toughness.

Generally, yield and tensile strengths correlated well with composition. As titanium increased, both yield and tensile strengths increased. Low- and high-temperature toughnesses, −46°C (−51°F) and +52°C (126°F), respectively, were dependent on all four elements, with titanium and manganese supplying the strongest effects. Decreasing the titanium and increasing the manganese increased the toughness. The toughness was also increased by decreasing the amount of proeutectoid ferrite and refining the microstructure.

A practical range of weld-metal toughnesses was found to be obtainable in titanium-bearing steels using appropriate combinations of electrode composition and flux basicity.

Introduction

Studies have suggested that small titanium additions up to an optimum level of about 0.04 wt-% can have a beneficial effect on the toughness of submerged arc weld metal (Ref. 1, 2, 3). Toughness though, appears to be continuously reduced by titanium additions greater than 0.04% indicating that high dilution welding processes such as submerged arc may develop low toughness weld deposits when used on base metals containing high titanium. However, as opposed to columbium and vanadium, titanium offers the combined advantage of greater metallurgical versatility and lower cost.

Specifically, titanium acts as a strengthener and sulfide-shape modifier, whereas columbium and vanadium have the strengthening function but do not control sulfide shape. As to the economics, columbium and vanadium cost about two and a half times more than titanium. For these reasons, the present study determined the effects of titanium up to 0.15 wt-% on the mechanical properties and microstructure in submerged arc weld deposits of high-strength low-alloy (HSLA) steels. In addition, the selection of consumables was examined as a means of countering the deleterious effect of higher titanium levels.

Experimental Program

To determine the effects not only of titanium variation but also the interaction of other elements with titanium, the design of the experimental program was factorial.

Twenty-one 227 kg (500 lb) laboratory ingots were poured and rolled to 13 mm (½ in.) thick plate to make up the two series of heats which were tested in this program. The chemistries of these heats are given in Table 1.

The first series, coded CTS, was chosen to fit a two-level three-factorial experimental design. These heats were based on variations in carbon, silicon, and titanium levels at a constant manganese level. The second series, coded CTM, was chosen to fit a partial factorial design based on variations in carbon, titanium, and manganese levels at a constant silicon level. Several of the heats provided base metal for both series as shown on Table 1.

Table 2 presents the compositions of the commercially produced welding electrodes and fluxes. A majority of the welds

Based on paper presented at the AWS 61st Annual Meeting in Los Angeles, California, during April 13-18, 1980.

J. P. SNYDER, II is an Engineer, Homer Research Laboratories, Bethlehem Steel Corporation, and A. W. PENSE is Professor and Chairman, Department of Metallurgy and Materials Science, Lehigh University, Bethlehem, Pennsylvania.

Table 1—Base Metal Chemistries, %

Plate	Series	C	Mn	P	S	Si	Ti	Al
1-S087	CTS	0.150	1.45	0.004	0.005	0.27	0.066	0.030
2-S060	CTS, CTM	0.120	1.48	0.004	0.005	0.53	0.100	0.050
3-S069	CTS, CTM	0.065	1.42	0.003	0.006	0.44	0.075	0.043
4-T107	CTS	0.072	1.49	0.006	0.003	0.24	0.075	0.037
5-W007	CTS	0.078	1.44	0.012	0.005	0.27	0.280	0.041
6-S071	CTS, CTM	0.062	1.53	0.003	0.005	0.51	0.270	0.041
7-S062	CTS, CTM	0.130	1.47	0.003	0.004	0.48	0.310	0.045
8-S091	CTS	0.130	1.54	0.003	0.005	0.31	0.330	0.040
9-T109	CTS	0.098	1.50	0.007	0.004	0.33	0.170	0.040
10-S064	CTS	0.130	1.29	0.003	0.005	0.27	0.170	0.036
11-S061	CTS, CTM	0.120	1.44	0.004	0.004	0.48	0.190	0.048
12-S070	CTS, CTM	0.071	1.52	0.003	0.005	0.49	0.160	0.039
13-S095	CTS	0.071	1.40	0.006	0.003	0.28	0.150	0.033
14-S066	CTM	0.130	0.92	0.003	0.006	0.40	0.065	0.037
15-S092	CTM	0.120	0.93	0.003	0.006	0.49	0.210	0.030
16-S068	CTM	0.130	0.96	0.003	0.005	0.46	0.260	0.026
17-S093	CTM	0.073	0.89	0.003	0.005	0.46	0.150	0.021
18-S094	CTM	0.130	0.97	0.002	0.006	0.29	0.170	0.024
19-W024	CTS	0.110	1.45	0.007	0.003	0.35	0.039	0.036
20-W058	CTS	0.067	1.46	0.003	0.004	0.23	0.002	0.042
21-W059	CTS, CTM	0.150	1.51	0.003	0.004	0.40	0.002	0.050

were made with electrode 123 and flux 85. Electrodes 128 and 130 were used to determine the effect of adding molybdenum or molybdenum plus nickel on the weld metal properties. Flux 851 and 0091 were used to determine the effect of flux basicity on weld metal properties.

Welding Procedure

All welding was done with a Scott-connected tandem AC submerged-arc system. Full-penetration welds of one pass per side were deposited into a square-butt joint. All plates were welded at a travel speed of 163 cm/min (i.e., 27.2 mm/s or 64 ipm) with an energy input of 21 kJ/cm (53.3 kJ/in.) using the following current (amperes, A) and voltage (volts, V) parameters: lead arc—900 A and 35 V; trail arc—600 A and 40 V.

This procedure resulted in the carbon, silicon, manganese and titanium values shown in Table 3. From the chemistries of both parent plate and weld metal, the titanium dilution was determined to be about 50%. The titanium dilution is shown graphically in Fig. 1.

Cooling rates were obtained from several of the welds by harpooning W-5% Re vs. W-26% Re thermocouples into the molten weld pool just in back of the trail electrode. Cooling rates for 10 such measurements had a mean value of 11.0°C/second(s) (19.8°F/s) between 800 and 500°C (1472 and 932°F) with a standard deviation of 0.5°C/s (0.9°F/s).

Testing and Metallographic Procedures

Specimens were removed for tensile and Charpy testing and chemical analysis as indicated in Fig. 2. Full-size Charpy specimens were machined transverse to the welding direction and notched in the plate thickness direction so as to contain about 60% of the second weld bead and about 40% of the first weld bead. Small, 0.5 inch (12.7 mm) gage length all-weld-metal tensile specimens were taken entirely from the second weld bead in the longitudinal direction.

Specimens for metallography and hardness testing were final-polished with 0.03 micron aluminum oxide powder and etched in 2% nital. Quantitative metallography was done with a Leitz texture analysis system.

Specimens for transmission electron microscopy (TEM) were taken from the second weld bead and mechanically polished to 0.40 mm (0.016 in.), chemically thinned to 0.05 mm (0.002 in.) in 5% hydrofluoric acid and 30% hydrogen peroxide in water followed by electrojet thinning in 10% perchloric acid in acetic acid at 12°C (54°F).

The scanning electron microscope and the electron microprobe were used, respectively, to examine the fracture surfaces of broken impact specimens and to qualitatively analyze inclusions on polished surfaces.

Results and Discussion

The first part of this study was a statistical analysis of chemistry effects on the mechanical properties of the weld metal. A stepwise regression program was employed to determine the relationships of several dependent variables to carbon, titanium, and silicon in the CTS welds and to carbon, titanium, and man-

Table 2—Welding Consumables, %

Electrode	C	Mn	P	S	Si	Mo	Ni	Ti	Al
123	0.12	1.97	0.012	0.024	0.03	0.004	0.04	0.004	0.008
128	0.15	1.89	0.011	0.017	0.05	0.50	0.05	—	0.035
130	0.16	1.91	0.006	0.013	0.07	0.42	0.84	0.004	0.008

Flux	SiO_2	Al_2O_3	TiO_2	CaO	MgO	MnO	FeO	Na_2O	CaF_2	BI[a]
85	39.3	5.5	18.6	20.7	0.4	13.0	0.9	0.05	2.2	0.59
851	42.8	2.6	11.5	37.5	0.4	0.4	0.4	0.05	4.5	0.85
0091	34.1	3.0	4.2	43.9	0.4	0.4	0.2	4.80	9.3	1.55

(a) Basicity index $= \dfrac{(CaO + CaF_2 + MgO + K_2O + 0.5[MnO + FeO])\ 0.5[MnO + FeO])}{(SiO_2 + 0.5[Al_2O_3 + TiO_2 + ZrO_2])}$

Table 3—Weld-Metal Chemistries, %[a]

Weld	C	Mn	P	S	Si	Ti	Al	O	N
1-S087	0.120	1.15	0.008	0.014	0.38	0.029	0.012	0.082	0.009
2-S060	0.100	1.37	0.006	0.012	0.60	0.077	0.039	0.085	0.009
3-S069	0.083	1.12	0.008	0.015	0.48	0.038	0.019	0.087	0.010
4-T107	0.070	1.30	0.010	0.011	0.37	0.036	0.020	0.083	0.019
5-W007	0.072	1.33	0.012	0.012	0.39	0.150	0.017	0.081	0.010
6-S071	0.063	1.39	0.008	0.012	0.55	0.110	0.022	0.087	0.012
7-S062	0.110	1.27	0.005	0.011	0.54	0.160	0.016	0.062	0.011
8-S091	0.110	1.41	0.007	0.012	0.47	0.160	0.017	0.072	0.008
9-T109	0.094	1.30	0.010	0.012	0.46	0.058	0.019	0.070	0.013
10-S064	0.110	1.18	0.005	0.012	0.38	0.090	0.012	NA[a]	0.009
11-S061	0.099	1.37	0.003	0.011	0.49	0.140	0.014	NA	0.012
12-S070	0.073	1.28	0.010	0.013	0.58	0.062	0.021	NA	0.013
13-S095	0.068	1.30	0.003	0.013	0.38	0.071	0.017	NA	0.012
14-S066	0.110	1.06	0.005	0.012	0.45	0.041	0.012	0.076	0.008
15-S092	0.110	1.09	0.006	0.013	0.58	0.080	0.010	NA	0.009
16-S068	0.110	1.07	0.006	0.012	0.54	0.130	0.015	0.077	0.008
17-S093	0.078	1.04	0.005	0.013	0.52	0.078	0.016	NA	0.008
18-S094	0.120	1.03	0.004	0.012	0.43	0.084	0.020	NA	0.009
19-W024	0.090	1.29	0.010	0.014	0.47	0.025	0.020	0.077	0.012
20-W058	0.066	1.31	0.005	0.014	0.36	0.009	0.026	0.091	0.009
21-W059	0.130	1.33	0.005	0.012	0.50	0.010	0.033	0.079	0.014

(a) NA—not analyzed.

ganese in the CTM welds. These variables were yield and tensile strengths, maximum hardness, Charpy V-notch energy, and Charpy energy transition temperatures for 20 and 55 J. The equation expressing the relationships was given the following form:

$$\text{Variable} = B_o + B_1C + B_2Ti + B_3Si + B_{11}C^2 + B_{22}Ti^2 + B_{33}Si^2 + B_{12}C \times Ti + B_{23}Ti \times Si + B_{13}C \times Si$$

where C, Ti, and Si equal the respective weight percentages in the weld metal for the CTS series. A similar equation was developed for the CTM series where manganese was substituted for silicon.

The regression program generated the coefficients, the multiple correlation coefficient (R), the standard error of the estimate (SErr), and the P-tail (P). The P-tail is the percent of the variability explained by chance, i.e., if P of an equation is equal to 0.02, then the relationship expressed by the equation has two chances out of one hundred of having occurred by chance.

Results of the analysis are given in Table 4. In the last column of Table 4, a correlation is defined as: "Excellent" if P of the equation is ≤ 0.01; "Good" if P of the equation is $0.01 < P \leq 0.05$; "Fair" if P of the equation is $0.05 < P \leq 0.15$; "Poor" if P of the equation is > 0.15.

With the exception of the CTM yield strengths, correlation was shown to be

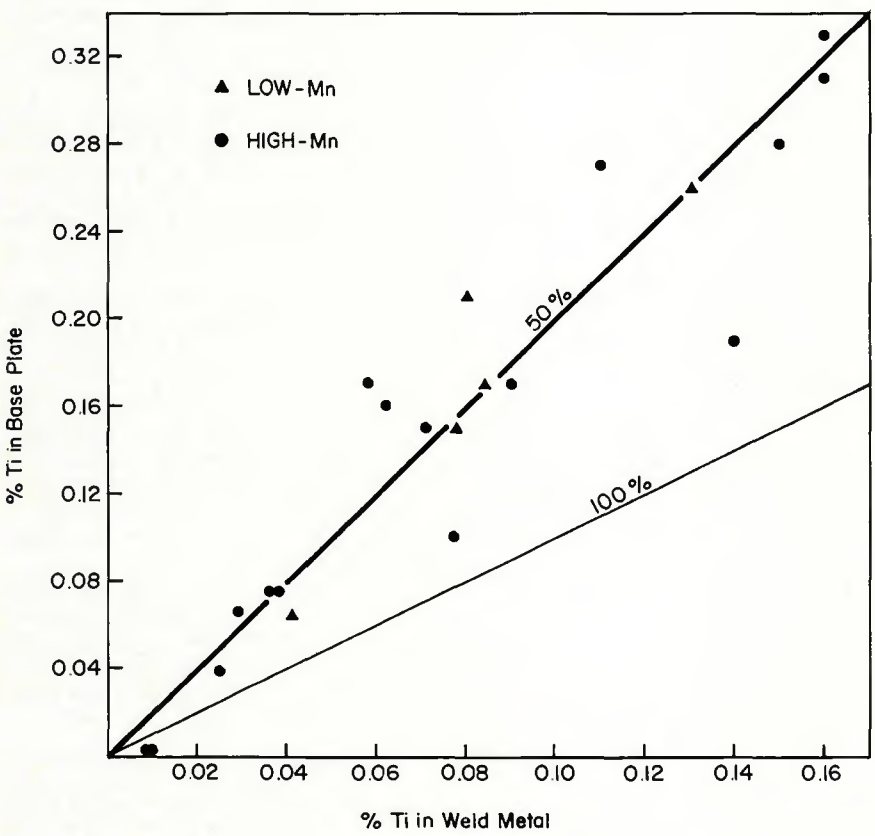

Fig. 1—Titanium dilution

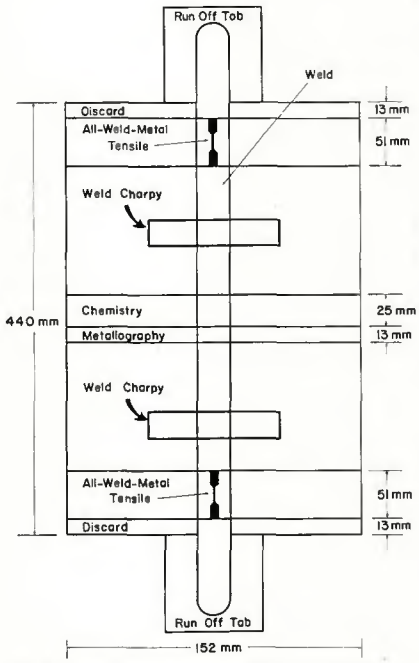

Fig. 2—Test plate and specimen location

Table 4—Results of Regression Analysis[a]

Variable	Units	Coefficients of equations										Statistical parameters			
		B_0	B_1	B_2	B_3	B_{11}	B_{22}	B_{33}	B_{12}	B_{32}	B_{31}	R	SE_{rr}	P	Correlation
CTS series:															
1 YSW	MPa	889.5	−10627.0	804.0	0	65758.8	0	812.0	12358.6	−3793.2	−4602.3	0.89	15.3	0.024	Good
2 TSW	MPa	707.3	−3826.4	534.8	0	29372.0	0	332.0	0	−696.8	−2269.7	0.92	11.1	0.003	Excellent
3 −46W	J	12.6	0	−91.3	0	0	480.9	0	−417.1	0	109.9	0.89	1.7	0.002	Excellent
4 −32W	J	39.4	−497.6	0	0	2208.3	−498.4	−27.8	0	0	382.6	0.96	1.8	0.001	Excellent
5 −18W	J	7.2	−239.6	−276.9	178.4	0	0	−254.9	0	−474.1	519.2	0.91	2.1	0.005	Excellent
6 +24W	J	86.4	0	−190.9	0	0	−5886.0	−222.3	0	0	2356.3	0.75	10.0	0.043	Good
7 +52W	J	156.9	−1170.8	−159.8	0	5007.4	0	0	983.0	0	0	0.86	4.4	0.010	Excellent
8 20JTT	°C	−4.9	0	265.2	−140.7	0	0	178.4	0	−349.6	−157.2	0.92	2.9	0.001	Excellent
9 55JTT	°C	3.3	0	146.4	0	0	0	0	0	0	−96.1	0.86	4.8	0.001	Excellent
10 MWH	HV5	178.6	219.4	314.4	0	0	0	0	−2232.3	0	0	0.82	4.8	0.003	Excellent
11 %V	%	−10.0	895.1	−106.5	−4.5	−5085.7	439.9	0	0	0	0	0.84	1.9	0.017	Good
CTM series:															
1 YSW	MPa	−58.4	6475.9	0	424.3	0	4481.2	0	−9676.8	0	−4693.9	0.69	23.4	0.440	Poor
2 TSW	MPa	435.1	0	2357.5	0	9291.9	0	140.2	0	−1850.8	−1155.0	0.93	9.2	0.012	Good
3 −46W	J	−16.4	0	0	27.5	0	521.1	0	0	−122.7	0	0.95	1.5	0.001	Excellent
4 −32W	J	0.3	0	−310.9	27.9	0	1092.3	0	0	0	−18.5	0.97	2.1	0.001	Excellent
5 −18W	J	76.1	0	−1373.7	−27.6	0	1436.2	0	0	830.5	0	0.95	3.5	0.001	Excellent
6 +24W	J	134.2	0	−2270.0	−38.0	0	1684.5	0	2005.3	1287.2	0	0.96	4.9	0.002	Excellent
7 +52W	J	−89.8	0	0	0	0	0	0	−1935.3	106.6	0	0.87	3.1	0.002	Excellent
8 20JTT	°C	−47.9	0	1429.4	0	0	−1978.5	0	0	−740.3	0	0.95	5.1	0.001	Excellent
9 55JTT	°C	−43.2	0	2274.6	32.5	0	0	0	−3135.0	−1395.4	0	0.96	4.9	0.001	Excellent
10 MWH	HV5	175.5	0	0	23.1	0	0	0	321.2	0	0	0.74	3.7	0.028	Good
11 %V	%	58.9	−614.1	718.7	−37.7	0	−910.5	0	0	−405.1	497.9	0.97	1.7	0.005	Excellent

[a] Notations are as follows:
CTS series: Variable = $B_0 + B_1(C) + B_2(Ti) + B_3(Si) + B_{11}(C^2) + B_{22}(Ti^2) + B_{33}(Si^2) + B_{12}(CTi) + B_{32}(SiTi) + B_{31}(SiC)$
CTM series: Variable = $B_0 + B_1(C) + B_2(Ti) + B_3(Mn) + B_{11}(C^2) + B_{22}(Ti^2) + B_{33}(Mn^2) + B_{12}(C.Ti) + B_{32}(MnTi) + B_{31}(MnC)$
Variables:
1) YSW – weld metal yield strength
2) TSW – weld metal tensile strength
3) −46W – weld metal CVN energy at −46°C
4) −32W – weld metal CVN energy at −32°C
5) −18W – weld metal CVN energy at −18°C
6) +24W – weld metal CVN energy at +24°C
7) +52W – weld metal CVN energy at +52°C
8) 20JTT – CVN 20J transition temperature
9) 55JTT – CVN 55J transition temperature
10) HWH – maximum weld metal hardness HV5
11) %V – ferrite veining

good on the basis of the P statistic as well as other statistical indices, including the multiple correlation coefficients. In the case of the yield strengths, the silicon level was more significant than the manganese level.

Since a ten-coefficient equation is not easily grasped, a series of graphs was plotted from the regression data. Figures 3 to 6 were selected from the results of the statistical analyses to graphically illustrate the most important effects of composition on mechanical properties. Although the effect of titanium on mechanical properties and microstructure is the main focus study, it is useful to first summarize the general effects of carbon, silicon, manganese, and titanium. The toughness, hardness, strength, and other data for the individual welds are given in Table 5.

Charpy Toughness. The transition temperature for 20 J ranged from −39 to +3°C (−38 to +37°F) and for 55 J ranged from −4 to +42°C (25 to 108°F). Titanium strongly increased and manganese strongly decreased the 55 J transition temperature – Fig. 3. Carbon and silicon had little effect on the transition temperature. Similar results were obtained for the 20 J transition temperature.

Charpy energies ranged from a low of 5 J at −46°C (−51°F) to a high of 106 J at +52°C (126°F). Energy increased with manganese and silicon and decreased with titanium and carbon. The effects of titanium and manganese were strong in comparison with those of carbon and silicon. Titanium and manganese strongly affected the absorbed energy at −18°C (0°F) – Fig. 4. Carbon and silicon had only a weak effect on absorbed energy at −18°C (0°F).

Hardness. Maximum Vickers hardnesses (5 kg load) ranged from 192 to 219 and increased with titanium, manganese, and carbon. However, the titanium and carbon effects were stronger than the manganese effect. The effect of silicon was weak.

Strength. Yield strengths ranged from 448 to 536 MPa (65 to 77.7 ksi) and the tensile strengths ranged from 570 to 648 MPa (82.7 to 94 ksi). Both the yield and tensile strengths were increased to various degrees by additions of titanium. Silicon raised yield strength a little but had almost no effect on the tensile strength. Manganese only slightly increased the yield strength but increased the tensile strength more strongly.

The trends are shown for tensile strength in Figs. 5 and 6. Figure 5 shows the tensile strength increasing with increasing titanium and carbon. Figure 6 shows the tensile strength increasing with manganese and carbon.

Effects of Titanium and Manganese

The strength of a factorial design is that it gives both main effects and interactions. The analyses showed that the

Table 5—All-Weld-Metal Data

Weld	Yield strength, MPa	Tensile strength, MPa	Charpy V-notch energy, joules −46°C	−32°C	−18°C	+24°C	+52°C	20 J transition temp., °C	55 J transition temp., °C	Maximum hardness, HV5	Ferrite veining, %	Inclusions, vol-%
1-S087	494	625	13	26	30	66	NT[a]	−37	7	209	20.4	0.64
2-S060	492	621	14	21	32	64	90	−34	13	212	21.4	0.60
3-S069	469	570	12	20	31	72	85	−31	10	208	22.5	0.56
4-T107	449	578	NT	22	30	74	95	−37	10	206	24.9	0.52
5-W007	495	612	9	11	20	51	87	−16	26	219	21.1	0.61
6-S071	519	619	9	16	30	61	95	−25	17	214	17.5	0.49
7-S062	500	625	8	13	27	61	79	−25	18	213	20.9	0.56
8-S091	527	648	11	14	28	53	81	−25	27	217	16.0	0.56
9-T109	470	596	14	22	32	72	92	−34	7	204	19.9	0.51
10-S064	507	615	8	17	25	72	85	−24	12	210	20.0	NM[b]
11-S061	450	596	7	12	32	76	79	−25	9	206	20.3	NM
12-S070	499	610	10	20	28	69	89	−32	12	203	20.1	NM
13-S095	488	590	9	20	29	75	90	−32	7	198	19.4	NM
14-S066	535	592	8	19	33	64	85	−30	12	200	18.9	NM
15-S092	514	609	5	8	12	51	80	−4	29	201	24.7	NM
16-S068	494	615	5	5	10	34	75	+3	42	206	32.4	NM
17-S093	482	586	5	10	13	43	89	−5	34	199	29.3	NM
18-S094	484	607	5	10	16	53	84	−11	24	204	27.6	NM
19-W024	452	588	15	24	35	109	NT	−37	−1	196	26.6	0.59
20-W058	482	583	15	19	35	89	106	−30	−3	192	23.5	0.58
21-W059	523	639	18	30	35	81	88	−39	−4	205	16.7	0.62

(a) NT—no test.
(b) NM—not measured.

strongest effects on toughness were caused by titanium and manganese, with carbon and silicon having only minor effects.

Charpy V-Notch Energy. Titanium was found to correlate well with the absorbed energy at all test temperatures and for both high (1.3%) and low (1.05%) manganese levels. As titanium increased, the toughness at −46°C (−51°F) decreased—Fig. 7. Also note that the lower manganese data points show lower toughness values than the higher manganese points. Data points on the graph are actual values taken from Tables 3 and 5.

The same trends of titanium decreasing and manganese increasing the toughness are evident at +52°C (126°F)—Fig. 8. As shown in Fig. 9, the 55 J transition temperature increased with increasing titanium and decreasing manganese contents.

Weld-Metal Hardness. The titanium trend found in the preceding three figures is partially explained in Fig. 10. The maximum weld hardness (Vickers with a 5 kg load) increased with titanium content, a result that is consistent with the findings of Boniszewski (Ref. 1) and Bauman (Ref. 4). They concluded that the titanium adversely affected the toughness of the weld deposit by increasing hardness through solid solution hardening with an attendant decrease in ductility. As Fig. 10 demonstrates, hardness increased with increasing manganese.

Figure 11 shows the relation between maximum hardness and the 55 J transition temperature. Toughness deteriorated as hardness increased. The observed effect of titanium on hardness can be attributed to solid solution hardening or, as noted later, to some precipitation effect.

Our results for the effects of titanium

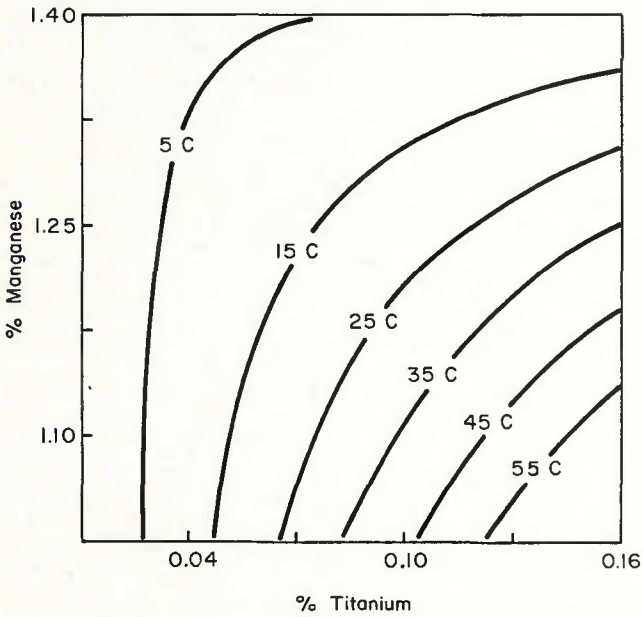

Fig. 3—55 joule transition temperature vs. titanium and manganese at 0.09% carbon (CTM series)

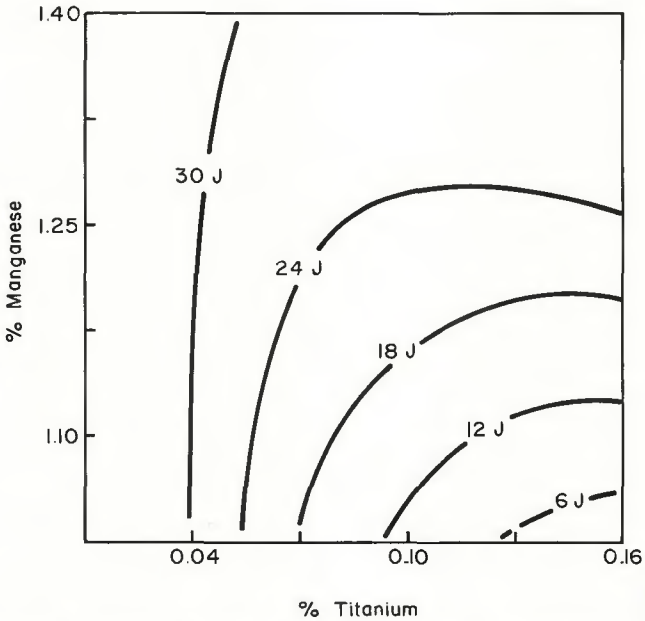

Fig. 4—Charpy V-notch energy at −18°C (0°F) vs. titanium and manganese at 0.09% carbon (CTM series)

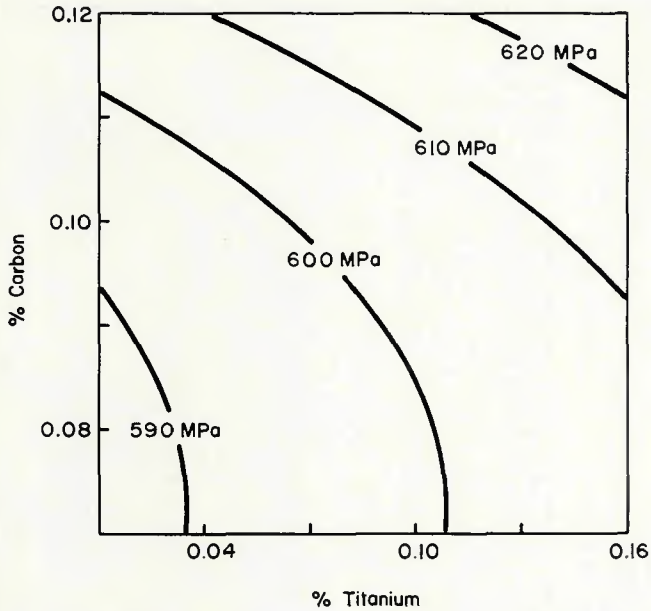

Fig. 5 — Tensile strength vs. titanium and carbon at 1.20% manganese (CTM series)

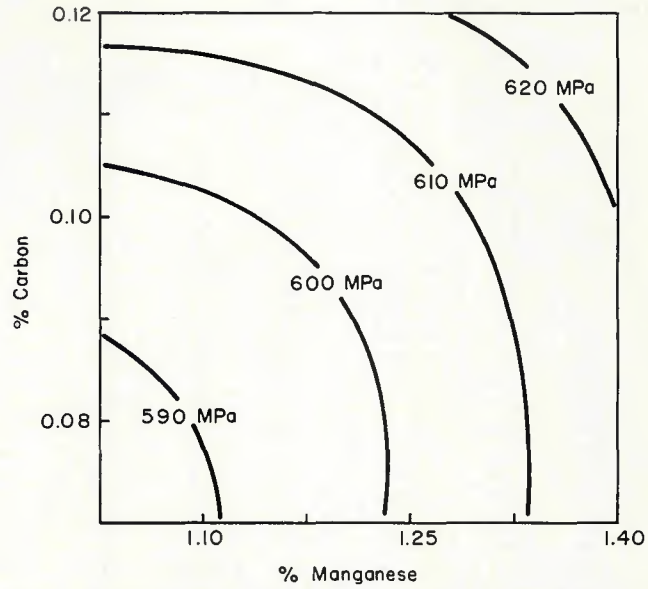

Fig. 6 — Tensile strength vs. manganese and carbon at 0.085% titanium (CTM series)

on toughness and hardness find support (Fig. 12) in Thaulow's study, in which the COD vs. Charpy toughness of submerged-arc welds was investigated at various titanium levels (Ref. 5).

Chemistry Effects on Microstructure

The microstructural features examined to explain the toughness variations were ferrite veining, inclusions, and ferrite grain size. Not all of these microconstituents were measured or statistically analyzed for each weld. Table 5 lists the collected data.

Ferrite Veining. Of all the transformation products found in carbon-manganese weld deposits, ferrite veining, or proeutectoid ferrite, is the most unambiguously recognized. Figure 13A shows a micrograph of ferrite veining at ×100. This veining surrounds areas of acicular ferrite, which forms at temperatures lower than that of the proeutectoid ferrite, as determined by Abson and Dolby (Ref. 6). Figure 13B shows acicular ferrite and a small area of ferrite veining (arrow). Microhardness measurements (10 gm load, kg/mm^2) given below show the acicular ferrite to be harder than the proeutectoid ferrite.

	Acicular	*Proeutectoid*
W058	201	154
S062	265	227

It is in the proeutectoid ferrite veins that cracks often initiate and propagate during Charpy testing. The polished cross section of a broken Charpy specimen in Fig. 14 shows the crack-propagation path to be through the ferrite veins. The embrittling effect of the veins results not from any inherent brittleness but rather from a mortar-in-brickwork morphology. The harder acicular ferrite concentrates the strain in the softer veins.

Titanium had differing effects on the amount of ferrite veining, depending on the level of manganese. The titanium

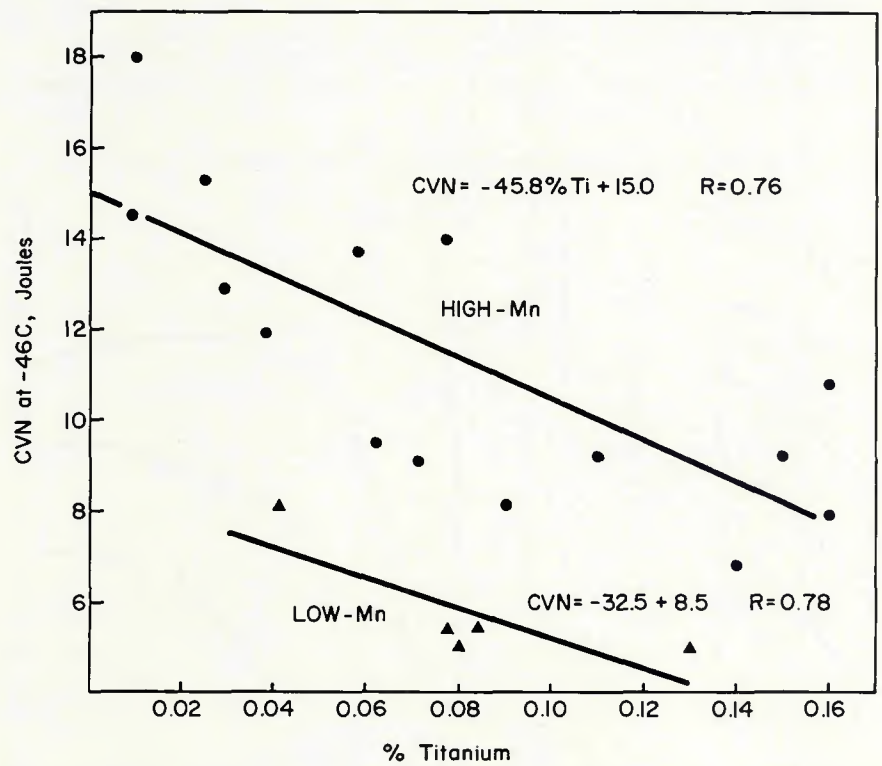

Fig. 7 — Charpy V-notch energy at −46°C (−51°F) vs. titanium. High Mn nominally 1.3%; low Mn nominally 1.05%. Equations are least-squares fit above and in following figures

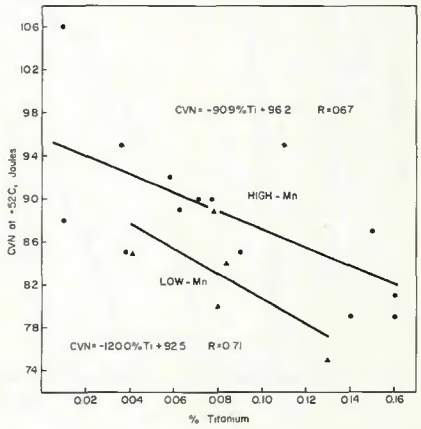

Fig. 8 — Charpy V-notch energy at 52°C (126°F) vs. titanium. High Mn nominally 1.3%; low Mn nominally 1.05%

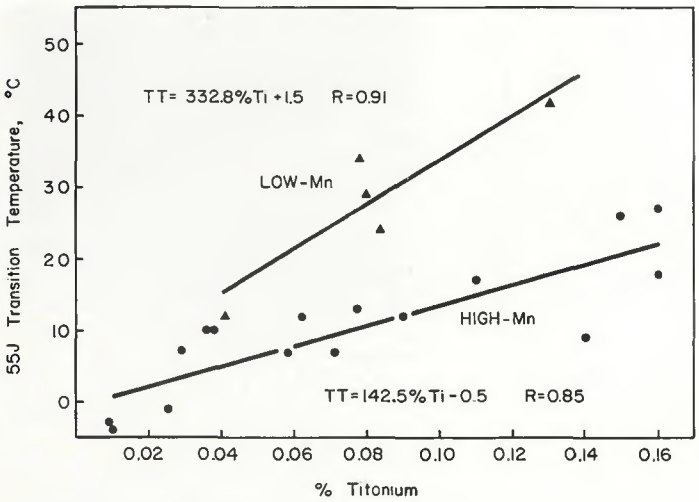

Fig. 9 — 55 joule transition temperature vs. titanium

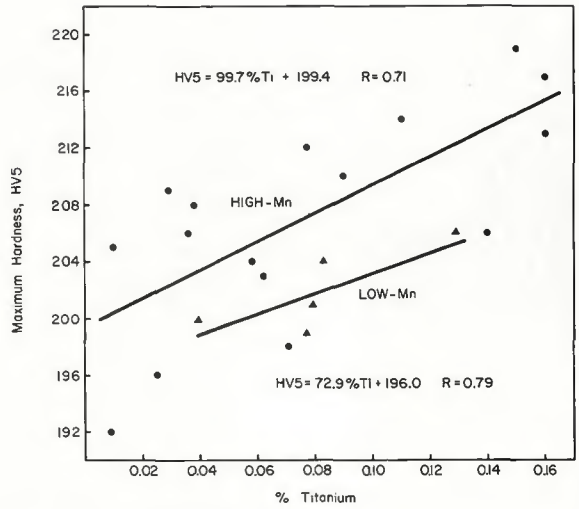

Fig. 10 — Maximum hardness vs. titanium

effect was weak at the higher manganese contents — Fig. 15. In contrast, at lower manganese levels, the relationship is such that as titanium increases the amount of ferrite veining increases — Fig. 16.

In one of his studies, Widgery noted that veining increased with increasing titanium (Ref. 2). Figure 17 shows that increased veining decreases the energy absorbed at +24 C. This deleterious effect of ferrite veining on toughness may also be accompanied by the adverse effect of increased hardness, as was shown in Fig. 10. Although the relation of toughness to veining is by no means a simple one, the practical point, as borne out by our own and other investigators' observations, is that good weld-metal toughness is obtained by avoiding proeutectoid ferrite in favor of acicular ferrite.

As evidenced by our results, when the manganese level is low, veining increases as the titanium increases — that is, there is a dichotomy in the effects of titanium on veining, depending on whether the manganese level is low or high. A possible explanation for this dichotomy is that the role of titanium as a ferrite promoter and stabilizer is overshadowed at the higher manganese levels where manganese effectively restricts the growth of grain-boundary ferrite and induces the formation of intragranularly nucleated ferrite.

Structure Size. Both titanium and manganese are known to refine the microstructure of base metals; they can also affect the weld deposit in a similar fashion. This effect is clearly shown for manganese in Fig. 18. The higher manganese content produced a finer microstructure than did the lower manganese content. Both compositions were similar except for the manganese.

According to Levin and Hill's classification (Ref. 7), Fig. 18A would be a category I structure due to the presence of acicular ferrite, and Fig. 18B would be a category II structure due to the lathlike morphology of the proeutectoid ferrite and the reduced amount of acicular ferrite. The higher manganese welds were also found to have a finer grain size in the weld metal heat-affected zone.

Titanium did not seem to have a well-defined effect on the structure size of the ferrite.

Inclusions. The volume percent (vol-%) of inclusions was measured for selected welds and compared to their oxygen contents. The inclusion data are found in Table 5. Since all welds to this point were made using an acid flux, the oxygen levels were similar at nominally 0.08%. The inclusion contents were also similar at about 0.5%.

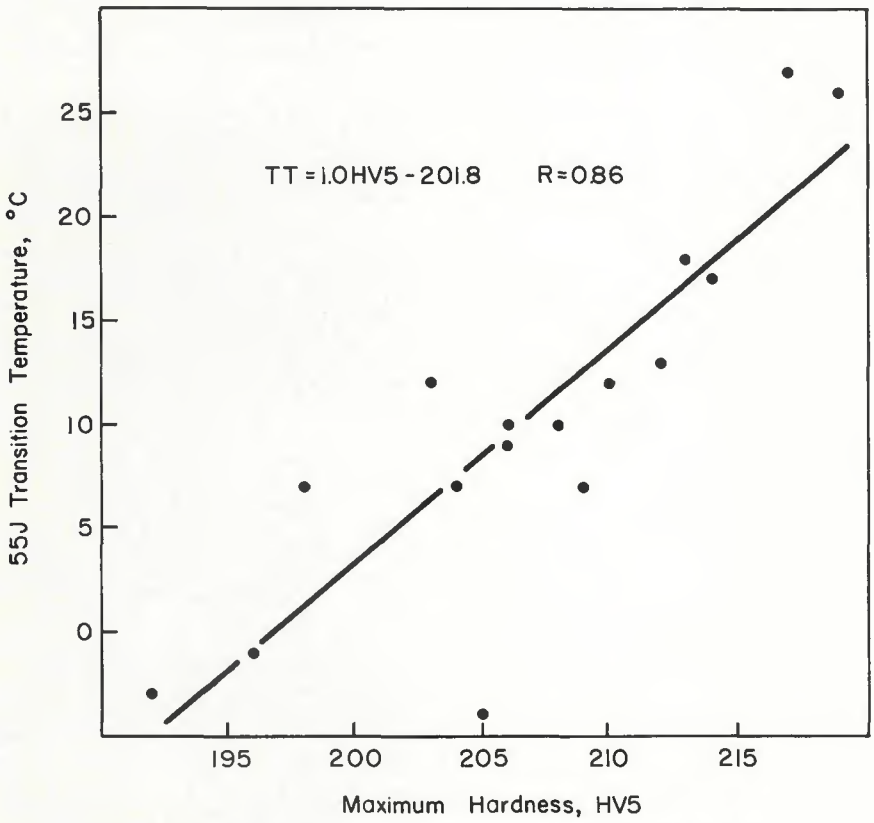

Fig. 11 — 55 joule transition temperature vs. maximum hardness. Mn nominally 1.3%

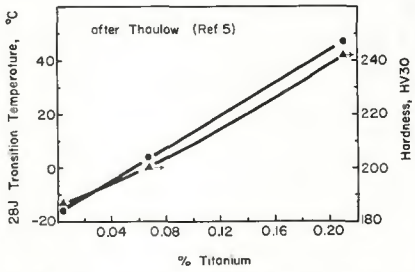

Fig. 12 — 28 joule transition temperature vs. hardness and titanium

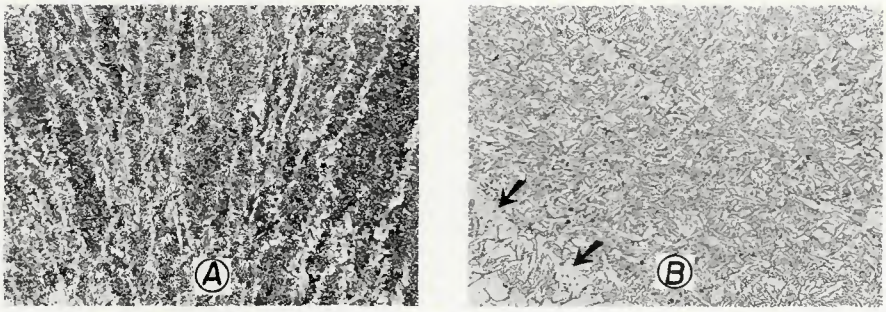

Fig. 13 — Microconstituents in a HSLA steel weld deposit: A — ferrite veining, ×100; B — acicular ferrite, ×500 (A and B reduced 48% on reproduction)

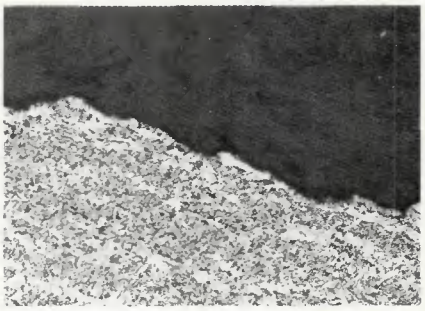

Fig. 14 — Crack-propagation path through ferrite veins

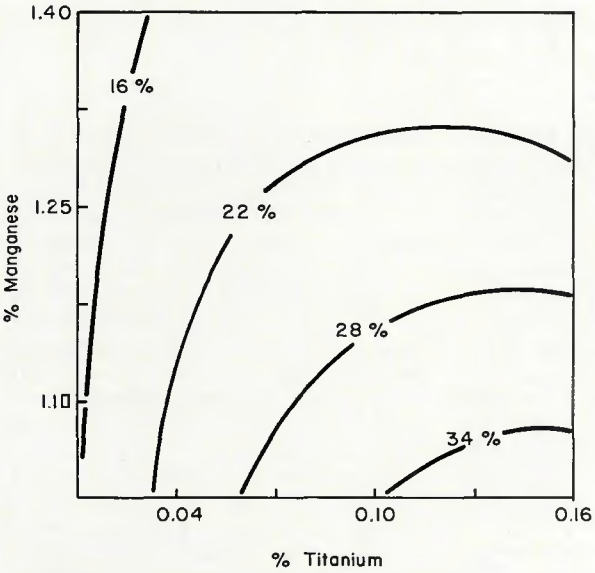

Fig. 15 — % ferrite veining vs. titanium and manganese at 0.07% carbon (CTM series)

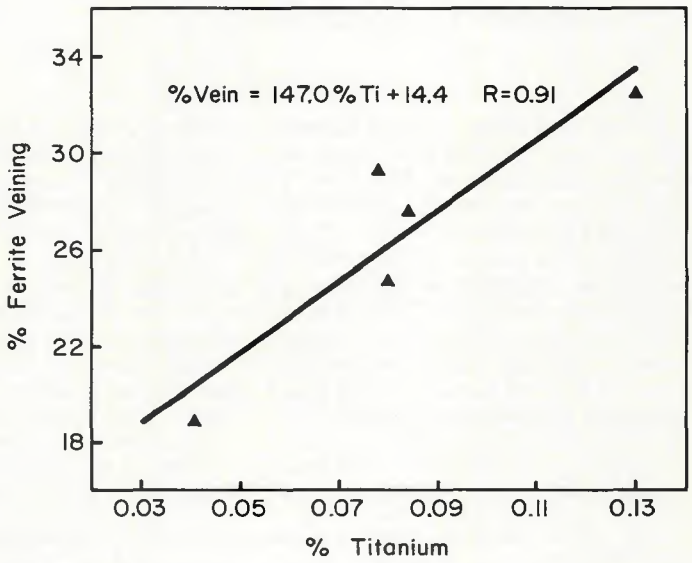

Fig. 16 — % ferrite veining vs. titanium for low-Mn welds. Mn nominally 1.05%

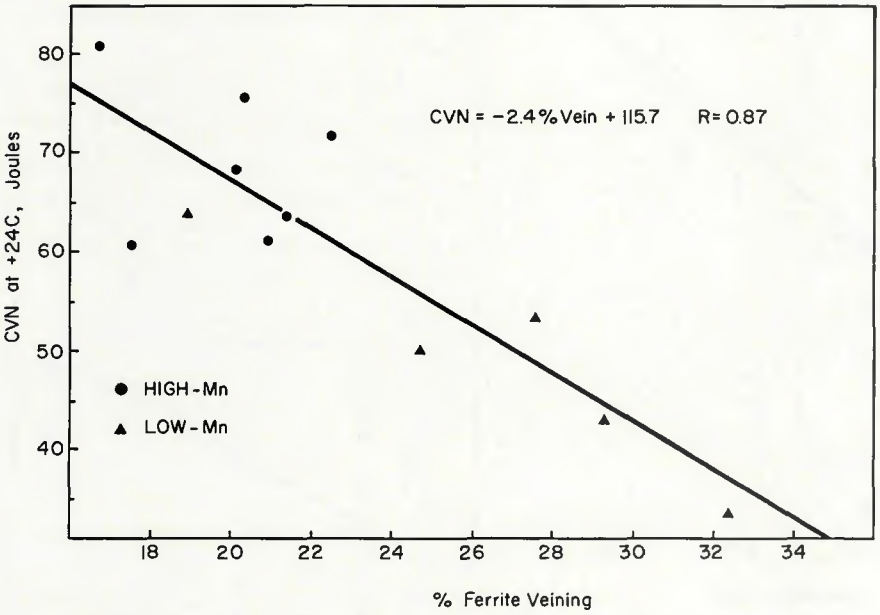

Fig. 17 — Charpy V-notch energy at +24°C (75°F) vs. % ferrite veining (CTM series)

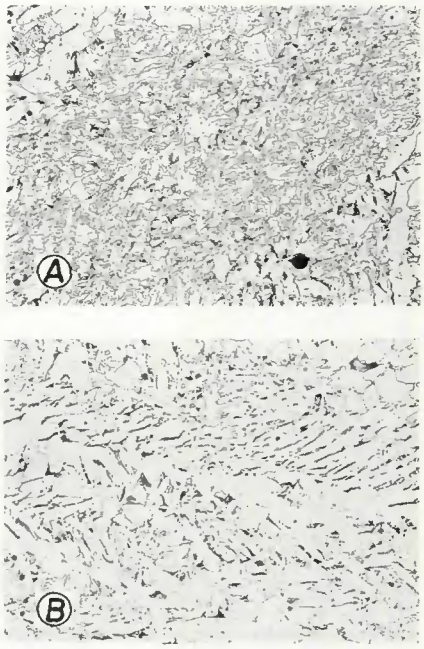

Fig. 18 — Effect of manganese on microstructure, −18°C (0°F): A — 1.27% Mn, 27 J; B — 1.07% Mn, 10 J. Nital etch; ×500 (reduced 48% on reproduction)

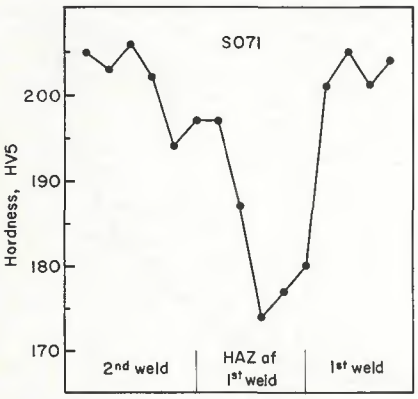

Fig. 19—Hardness vs. position in the weld deposit

Qualitative microanalysis showed that inclusions were mainly oxides, some sulfides also being present. Since the type and quantity of inclusions were all similar, their effect on properties and microstructures was not measurable. However, as discussed in a later section, quantity of inclusion can have a strong effect on Charpy energy.

Hardening Mechanism. Some investigators attribute the relationship between increased hardness and decreased toughness in a weld to precipitation hardening caused by carbides and nitrides (Ref. 8–10). However, their studies present no electron microscopic evidence of the presence of such precipitates. Consequently, precipitates other than these should be considered.

For example, the relationship between titanium and hardness in the present study might be explained by the formation of fine titanium carbides or nitrides, typical of experience in base metals. However, transmission electron microscope work, both thin-foil and extraction replicas, revealed no particles except for iron carbides which were associated with fine pearlite throughout the weld deposit. Scanning transmission electron microscope (STEM) work on thin foils revealed small titanium-aluminum oxide particles dispersed throughout the matrix but no titanium nitrides or carbides.

An attempt was made to extract particles by dissolving the matrix, and collecting and x-ray analyzing the residue according to Kreige's procedure (Ref. 11). The only particles thus obtained were oxides. As such evidence indicates, the higher oxygen contents of the weld metal would cause the titanium to be fixed as oxides rather than carbides or nitrides which develop in the base metal with its characteristically lower oxygen contents.

Thermodynamic data show that titanium carbides and nitrides are less stable than titanium oxides (Ref. 12, 13). Also, a hardness increase is typically found in the first weld bead where carbides and nitrides are active due to the aging in the first weld deposit that is caused by the heat of the second weld pass. Hardness traverses made from the second weld bead into the first weld bead showed no evidence of increased hardness—Fig. 19. The hardness decrease is due to the formation of stress-free polygonal ferrite.

As evidenced by these findings—in particular, by the absence of titanium nitrides or carbides as well as by the absence of a hardness increase—a carbide or nitride precipitation mechanism was ruled out in our study. On the other hand, the oxides found in the STEM work and the evidence of the type presented in Fig. 10, 15, and 19 point to the deleterious effect of titanium being due to dispersion hardening by oxide particles and, as discussed previously, to increased veining at low-manganese levels.

Effect of Flux Variation

For linepipe welding, acid fluxes have been popular because they produce sound, smoothly contoured deposits and have good operating characteristics at the high current levels and travel speeds typical of the application (Ref. 14, 15, 16). Unfortunately, acid fluxes produce high oxygen contents in the weld metal, an effect that is deleterious to notch toughness.

To determine acceptable oxygen levels, three fluxes of varying basicities were tried with a carbon-manganese electrode to produce welds on a medium-titanium plate. Generally, the higher the basicity, the lower the oxygen level and the higher the toughness—Fig. 20. As the basicity of the flux increased, the absorbed energy increased, especially near the upper shelf.

The data in Fig. 21 confirm the basicity/oxygen relation, and Fig. 22 shows that as the oxygen decreased, the volume-percent of inclusions decreased. From previous work done on fracture surfaces, it is known that fewer inclusions produce larger dimples on a ductile fracture surface due to the smaller number of inclusions available to initiate microvoid coalescence (Ref. 17, 18). Figure 23 shows scanning electron micrographs from Charpy specimens of high and low oxygen deposits. The larger dimple size of the lower-oxygen weld indicates a higher energy absorption.

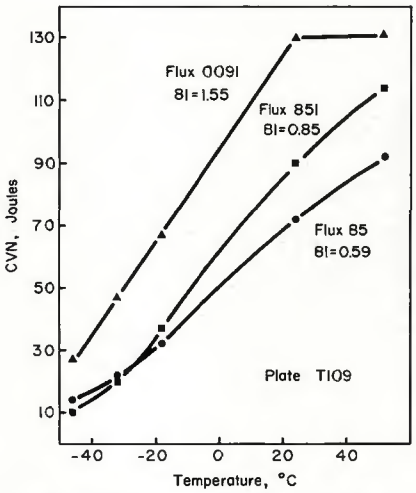

Fig. 20—Charpy energy curves for 85, 851, and 0091 fluxes

The literature also shows that as oxygen is decreased, the microstructure tends to have a higher percentage of acicular ferrite. This trend, although weak, was found for the flux series of welds. Figure 24 shows the microstructures of the high and low oxygen welds with their respective percents of ferrite veining and oxygen contents. The lower oxygen deposit is seen to contain less ferrite veining than the higher oxygen deposit. Investigators (Ref. 16, 19, 20) have suggested that oxide inclusions enhance transformation at the prior austenite grain boundaries and favor proeutectoid ferrite formation over acicular ferrite, which transforms intragranularly at a slightly later time.

Effect of Electrode Variation

Some investigators have indicated that additions of molybdenum or molybdenum plus nickel improve weld-metal toughness by reducing the amount of ferrite veining. To determine the effect of molybdenum and nickel on weld metal that contains titanium, several welds were made with electrodes of carbon-manganese, carbon-manganese plus molybdenum, and carbon-manganese plus

Table 6—Weld Metal Data: Electrode Variations

Weld/electrode	Ti, %	Charpy V-notch energy, joules −46°C	Charpy V-notch energy, joules +24°C	Transition Temp., °C	Ferrite veining, %
7-S062/123	0.16	8	61	18	20.9
7-S062/128	0.14	24	69	15	10.5
7-S062/130	0.09	28	78	11	7.1
21-W059/123	0.01	18	81	−4	16.7
21-W059/128	0.01	28	94	−10	3.8

Fig. 21—Oxygen content of weld metal vs. flux basicity

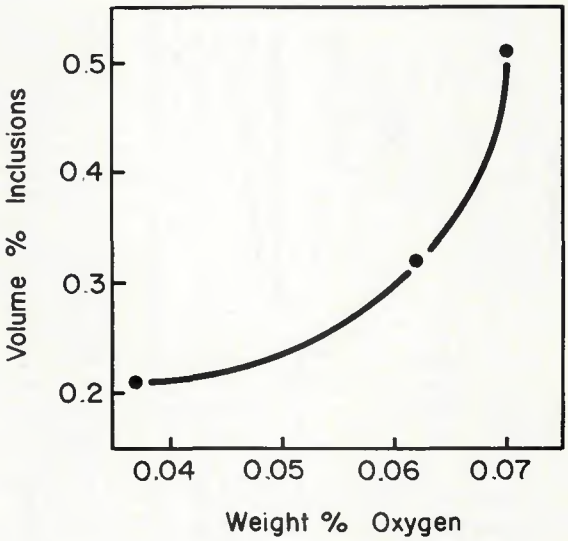

Fig. 22 (right)—Volume of inclusions vs. weld metal oxygen content

molybdenum and nickel. The 85 flux was used because of its superior operating characteristics, particularly for linepipe. As the two elements were added, the toughness was improved—Table 6.

The improvement in toughness is due to the increased hardenability supplied by molybdenum and nickel; this, as seen in Fig. 25, suppressed the formation of the ferrite veining and replaced it with acicular ferrite. This effect is consistent with the findings of Yoshino and Stout (Ref. 21) and of Takahashi (Ref. 22). Note that the decrease in veining with the concomitant increase in acicular ferrite is sufficient to maintain toughness even though there is an increase in hardness and strength. The explanation is that the shift in favor of acicular ferrite means a reduction in the amount of structure having a mortar-in-brickwork morphology, and therefore a reduction in the availability of crack-propagation paths.

The effect of molybdenum is active at both high and low titanium levels, as evidenced by welds W059 and S062—Table 6. However, the deleterious effect of titanium is also active in the presence of molybdenum, as is seen in a comparison of welds S062 and W059.

Conclusions

The findings of this study demonstrate that the detrimental effect of titanium on the toughness of submerged-arc welds in HSLA steels can be offset by the proper selection of electrode composition and flux basicity. Specifically, the study showed that:

1. Toughness is strongly dependent on the titanium and manganese levels. The toughness increases with decreasing titanium and increasing manganese. Titanium increases the amount of ferrite veining at low manganese levels and also increases the maximum weld-metal hardness through dispersion hardening. Manganese decreases the amount of ferrite veining and refines the microstructure. Carbon and silicon have comparatively

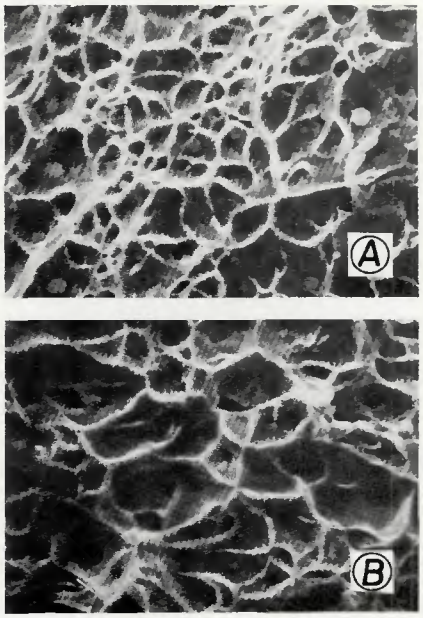

Fig. 23—Scanning electron micrographs of broken Charpy specimens, +52°C (126°F): A—0.070% oxygen, 92 J; B—0.037% oxygen, 131 J. ×2000 (reduced 41% on reproduction)

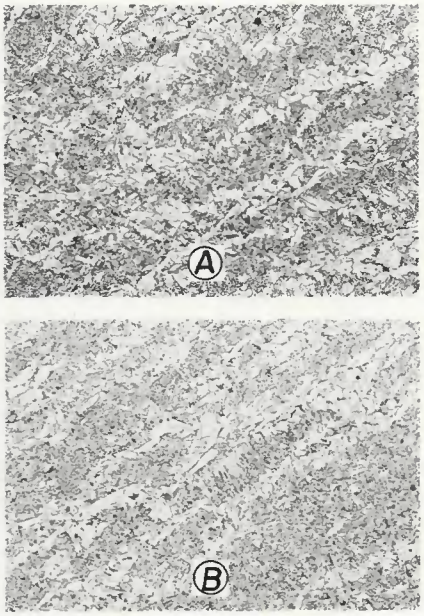

Fig. 24—Effect of oxygen on the amount of ferrite veining: A—0.062% oxygen, 21.1% veining. B—0.037% oxygen, 15.3% veining. Nital etch, ×200 (reduced 48% on reproduction)

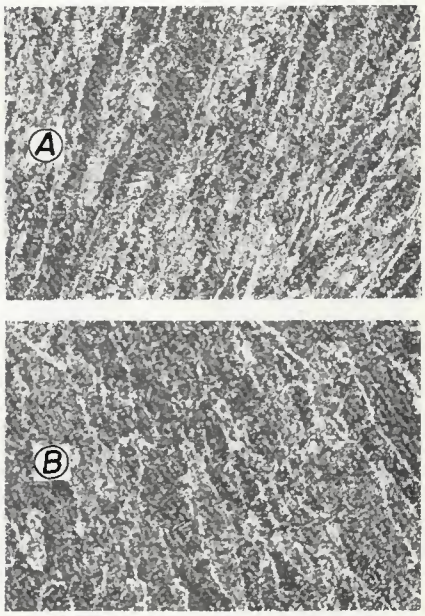

Fig. 25—Effect of molybdenum in reducing the amount of ferrite veining; A—0% molybdenum, 16.7% veining; B—0.15% molybdenum, 3.8% veining. Nital etch, ×100 (reduced 48% on reproduction)

weak effects, with carbon decreasing and silicon increasing the toughness.

2. Toughness is improved by using higher-basicity fluxes. These fluxes reduce the oxygen level with a concomitant reduction in inclusion volume. Also, ferrite veining is reduced slightly with the higher-basicity fluxes.

3. Molybdenum or molybdenum plus nickel additions improve toughness by reducing the amount of ferrite veining.

4. Maximum hardness increases with titanium, manganese, and carbon contents. The effect of silicon is weak.

5. Yield and tensile strengths increase with carbon, manganese, silicon, and titanium content. Manganese and silicon have comparatively weak effects on, respectively, yield and tensile strength.

Acknowledgments

The authors would like to express their appreciation to Messrs. Bauer, Benscoter, Brandemarte, and Kilpatrick for their skillful assistance throughout this program. The editorial comments of B. S. Mikofsky are greatly appreciated.

References

1. Boniszewski, T. 1969 (May). Titanium in steel wires for CO_2 welding. *Metal Construction* 1(3):225–229.

2. Widgery, D. J. 1974. Deoxidation practice and toughness of mild steel weld metal. *Welding Research International* 4(2):54–80.

3. Ito, Y., and Nakaniski, M. 1976 (May). Study on Charpy impact properties of weld metal with submerged-arc welding. *Sumitomo Search No. 15*:42.

4. Bauman, S. F., et al. 1977 (March). Wire and flux development for seam welding of HSLA line pipe. *Welding of line pipe steels:* 56–85. WRC Monograph.

5. Thaulow, C. 1979. Comparison between COD at initiation of ductile crack growth and maximum load of submerged-arc weld metal. *Int. Journ. of Fracture* 15:R31 to R35.

6. Abson, D. J., and Dolby, R. E. 1978 (July). Microstructural transformations in steel weld metals. *Welding Institute Research Bulletin* 19(7):202 to 207.

7. Levin, E., and Hill, D. C. 1977 (September). Structure-property relationships in low-C weld metal. *Met. Trans.* 8A:1453–1463.

8. Levin, E., and Hill, D. C. 1976 (February). *A review of the structure and properties of welds in columbium- or vanadium-containing high strength low alloy steels.* WRC Bulletin No. 213.

9. Signes, E. G., and Baker, J. C. 1979. Effects of columbium and vanadium on the weldability of HSLA steels. *Welding Journal* 58(6):179-s to 187-s.

10. Jessman, R. J. 1975. Columbium pickup in high-dilution submerged-arc weld deposits. *Proceedings of microalloying 75:*74 to 87.

11. Kriege, O. H. 1973. *Metallography—a practical tool for correlating the structure and properties of materials:* 220. ASTM-STP 557.

12. Comstock, G. F., et al. 1949. *Titanium in steel:* 70. New York: Pitman.

13. Skinner, G., et al. 1954. *Titanium and its compounds:* 21. Columbus, Ohio: Johnston.

14. Bailey, N., and Davis, M. L. E. 1977 (May). *Fluxes for submerged-arc welding ferritic steels—a literature survey.* Welding Institute Research Report 38/1977/M.

15. Jackson, C. E. 1973 (December). *Fluxes and slags in welding.* WRC Bulletin No. 190.

16. Garland, J. G., and Bailey, N., *The formulation and properties of submerged-arc welding fluxes.* Brit. Steel Corp. Rep. GS/PROD/498/1/74/C.

17. Broek, D. 1973. Roll of inclusions in ductile fracture. *Engineering Fracture Mechanics* 5(1):55–66.

18. Eriksson, K. 1975. Fracture toughness and the distribution of inclusion. *Scand. Jour. of Meta.* 4:173–176.

19. Abson, D. J., et al. 1978 (November 14). The role of non-metallic inclusion in ferrite nucleation on carbon steel weld metals. *Trends in steel and consumables for welding:* 75. London.

20. Cochrane, R. C., and Kirkwood, P. R. 1978 (November 14). The effect of oxygen on weld metal microstructure. Ibid: 103.

21. Yoshino, Y. and Stout, R. D. 1979. Effect of microalloys on the notch toughness of line pipe seam welds. *Welding Journal* 58(3):59-s to 68-s.

22. Takahashi, N., et al. 1977 (March). Developments for seam welding of high test line pipe. *Welding of line pipe steels:* 36 to 55. WRC Monograph.